

Superconducting Contact Geometries for Next-Generation Quantized Hall Resistance Standards

Alireza R. Panna*, Mattias Kruskopf*,[‡], Albert F. Rigosi*, Martina Marzano*,^{‡,1}, Dinesh K. Patel*, Shamith U. Payagala*, Dean G. Jarrett*, David B. Newell*, and Randolph E. Elmquist*

*National Institute of Standards and Technology, 100 Bureau Drive, Stop 8171, Gaithersburg, MD, 20899, USA
alireza.panna@nist.gov

[‡]Physikalisch-Technische Bundesanstalt, Department of Electrical Quantum Metrology, Braunschweig, 38116, Germany

¹Istituto Nazionale Di Ricerca Metrologica, Torino 10135, Italy

Abstract — Precision quantum Hall resistance measurements can be greatly improved when implementing new electrical contact geometries made from superconducting NbTiN. The sample designs described here minimize undesired resistances at contacts and interconnections, enabling further enhancement of device size and complexity when pursuing next-generation quantized Hall resistance devices.

Index Terms — quantum Hall effect, quantized Hall resistance standards, epitaxial graphene, multi-series electrical contacts.

I. INTRODUCTION

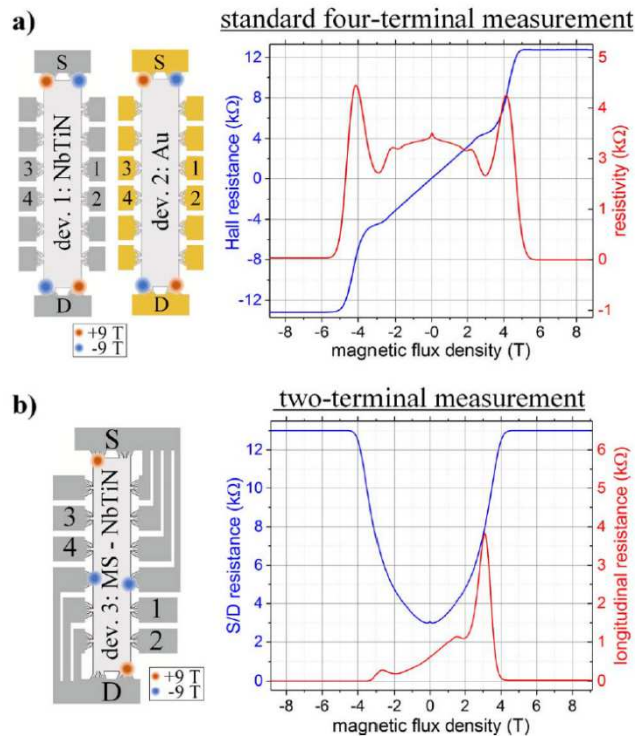
The quantum Hall effect in graphene devices have recently allowed for robust resistance plateaus ($R_H = R_K/2 = h/2e^2$) to be used as a metrological realization of the ohm [1]. One future avenue for dissemination of the ohm is through the construction of quantum Hall array resistance standards that are able to provide multiple quantized resistance values [2]–[6]. Before such networks can be fabricated, accumulated resistances at contacts and interconnections must be reduced. In this work, quantized Hall resistances (QHR) of epitaxial graphene devices are measured and compared using both the four-terminal and two-terminal approach. Undesired resistances were significantly reduced when superconducting multi-series contacts were applied. These new device contact geometries and compositions open new routes in the design of next-generation resistance standards.

II. PREPARATION OF DEVICES AND INITIAL COMPARISON

The device fabrication process is well documented in recent work [5]–[7]. After a NbTiN layer is sputtered onto a Ti adhesion layer, it is capped with Pt to prevent oxidation. The finished devices were functionalized with chromium tricarbonyl [$\text{Cr}(\text{CO})_3$] for tunable and uniform doping without the need for electrostatic gates [8]. For the sake of comparison, some devices were fabricated with Au electrical contacts. Preliminary measurements were then performed to assess the two-terminal versus four-terminal device responses.

In Fig. 1. (a), what are labelled as device 1 (using NbTiN contacts) and device 2 (using Au contacts) represent typical devices for standard four-terminal QHR measurements. The corresponding magnetic field sweep of device 1 shows the

Hall resistance (blue curve), with the Hall plateaus converging at high fields above ± 5.5 T. In Fig. 1 (b), device 3 (NbTiN contacts) uses a multi-series connection for the two-terminal measurements, further reducing longitudinal resistance

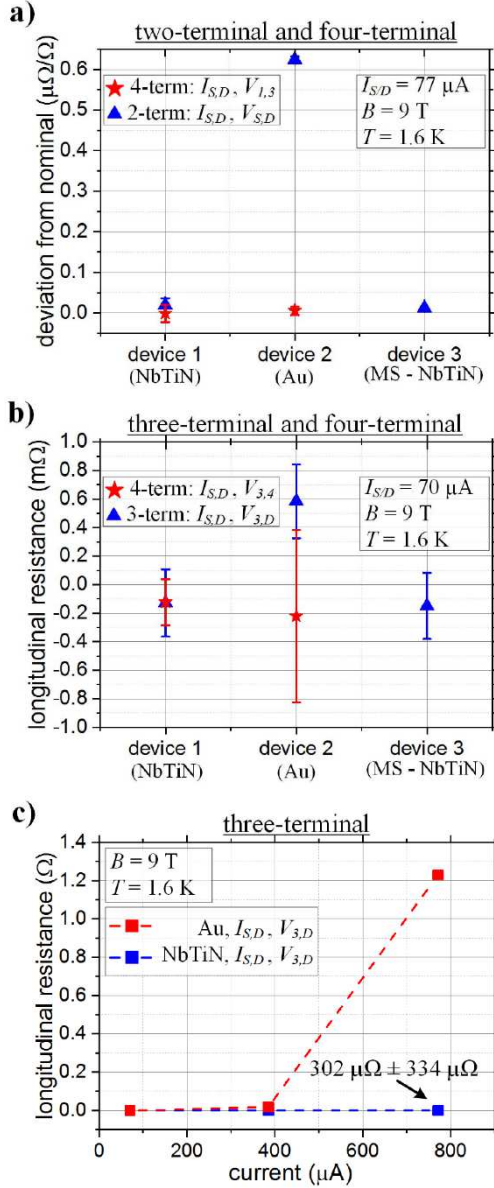


contributions while operating at 9 T.

Fig. 1. (a) An illustration of part of devices 1 (NbTiN) and 2 (Au) is provided along with its corresponding four-terminal measurement. The hot spots for the positive and negative magnetic flux densities are shown in red and blue. (b) The illustration for device 3 (only NbTiN) shows the used multi-series connection for two-terminal measurements to eliminate longitudinal resistance contributions [6]. Hot spots are marked in red and blue for positive and negative magnetic flux densities, respectively. © 2019 IEEE. Reprinted, with permission, from Ref. [6].

In the two-terminal configuration, the magnetoresistance is symmetric. The longitudinal resistance is asymmetric with magnetic field direction, and this arises from differences in the

current path. The hot spots in the quantum Hall regime are marked in the red and blue for positive and negative magnetic flux densities.



III. CONTACT ASSESSMENT

Fig. 2. (a) CCC and DCC QHR measurements. The pin labels match those in Fig. 1. These data assess the viability of two-terminal versus four-terminal measurements and compare the use of Au and NbTiN as contact metals. (b) The corresponding longitudinal resistances are shown for the same devices. The error bars indicate the standard deviation of the measurements. (c) Three-terminal longitudinal resistance measurements are shown bearing no significant current dependence for currents as high as $770 \mu\text{A}$. © 2019 IEEE. Reprinted, with permission, from Ref. [6].

Contact resistance improvements shown in Fig. 2. (a) were assessed with a cryogenic current comparator (CCC) for device 2 (Au) and 3 (MS-NbTiN) and direct current comparator (DCC) for device 1 (NbTiN). In Fig. 2. (a), precision QHR measurements show the deviation of the resistance from its nominal value of $R_{K/2} = h/2e^2 \approx 12906.4 \Omega$. Devices 1 and 2 were measured with both four-terminal (red stars) and two-terminal (blue triangles) configurations whereas device 3 was measured with only the two-terminal configuration. The used pin labels in the Fig. 2 legend correspond to those in Fig. 1. In the two-terminal configuration, the deviations from nominal are of the order $10 \text{ n}\Omega/\Omega$ and $600 \text{ n}\Omega/\Omega$ when using NbTiN and Au contacts, respectively

In Fig. 2 (b), longitudinal resistance measurements on the low potential side of the Hall bar were performed by applying a DC current with reversals and using a nanovoltmeter. The values were determined by measuring the voltage drop between neighboring Hall contacts using four terminals (red stars) as well as between a Hall contact and the drain contact using a three-terminal configuration (blue triangles). The three-terminal longitudinal resistance across the drain contact vanished, indicating a small effective contact resistance for the cases of device 1 and 3. In Fig. 2 (c) the two contact metals are compared using three-terminal resistance measurements. In the case of NbTiN contacts, no significant current dependence occurs for currents as high as 0.77 mA , whereas the Au counterpart encounters current dependence near 0.5 mA . This enables the use of a 50 % larger current in the device.

IV. CONCLUSION

We have demonstrated that the use of multi-series contacts allows for voltage and resistance measurements to be unaltered by contact resistances. Moreover, the use of superconducting material further reduces undesired resistances to enable simple, crossover-free interconnections. These improvements may accelerate future device design for resistance standards that depend upon such series and parallel elements.

REFERENCES

- [1] A. F. Rigosi *et al.*, "The quantum Hall effect in the era of the new SI," *Semicond. Sci. Technol.*, 34, 9, 093004, 2019.
- [2] A. Lartsev, *et al.*, "A prototype of $R_K/200$ quantum Hall array resistance standard on epitaxial graphene," *J. Appl. Phys.*, vol. 118, no. 4, p. 044506, Jul. 2015.
- [3] S. Novikov *et al.*, "Mini array of quantum Hall devices based on epitaxial graphene," *J. Appl. Phys.*, vol. 119, no. 17, p. 174504, May 2016.
- [4] M. Marzano *et al.*, "Implementation of a graphene quantum Hall Kelvin bridge-on-a-chip for resistance calibrations," *Metrologia*, 57, 1, 015007, 2020.

- [5] M. Kruskopf *et al.*, “Next-generation crossover-free quantum Hall arrays with superconducting interconnections,” *Metrologia*, 56, 6, 065002, 2019.
- [6] M. Kruskopf *et al.*, “Two-terminal and multi-terminal designs for next-generation quantized Hall resistance standards: contact material and geometry,” *IEEE Trans. Electron Dev.*, 66, 9, 3973-3977, 2019.
- [7] A. F. Rigosi *et al.*, “Electrical Stabilization of Surface Resistivity in Epitaxial Graphene Systems by Amorphous Boron Nitride Encapsulation,” *ACS Omega*, 2, 2326 – 2332, 2017.
- [8] A. F. Rigosi *et al.*, “Gateless and reversible Carrier density tunability in epitaxial graphene devices functionalized with chromium tricarbonyl,” *Carbon*, 142, 468–474, 2019.